The intrinsic nanofibrillar morphology of polyaniline

Jiaxing Huang† and Richard B. Kaner*

Received (in Cambridge, UK) 3rd August 2005, Accepted 31st October 2005
First published as an Advance Article on the web 6th December 2005
DOI: 10.1039/b510956f

Polyaniline nanofibers are shown to form spontaneously during the chemical oxidative polymerization of aniline. The nanofibrillar morphology does not require any template or surfactant, and appears to be intrinsic to polyaniline synthesized in water. Two approaches—interfacial polymerization and rapidly-mixed reactions—have been developed to prepare pure nanofibers. The key is suppressing the secondary growth that leads to agglomerated particles. The effects of different dopant acids and solvents are discussed. Changing the dopant acid can be used to tune the diameters of the nanofibers between about 30 and 120 nm. Changing the organic solvent in interfacial polymerization reactions has little effect on the product. A brief discussion of the processibility of the nanofibers is presented. The possibility of creating nanofibrillar structures for selected polyaniline derivatives is also demonstrated.

Introduction

Polymer nanostructures,[1–3] particularly conducting polymer nanowires and nanofibers,[4–6] have received growing interest in recent years. Conducting polymer nanofibers present a "soft", organic model for studying one-dimensional systems at the nanometer scale, and hold great promise as active components for nanoscale molecular electronic devices. Conventional conducting polymers are already being used and/or examined for many applications including in batteries, sensors, actuators, catalysts, electromagnetic shielding, antistatic coatings, corrosion protection, separation membranes, electro-optic and electrochromic devices.[7,8] It is therefore of both great technological and scientific interest to investigate whether nanostructures of conducting polymers can lead to better performance in these already established areas, and to ask if they can create new opportunities. Therefore, reliable and scalable synthetic methods for conducting polymer nanostructures must be developed in order to provide the necessary materials base for both research and applications.

Polyaniline is unique among the family of conducting polymers due to its ease of synthesis, environmental stability and simple doping/dedoping chemistry.[9–11] Polyaniline is usually made by the chemical oxidative polymerization of aniline using a strong oxidant such as ammonium peroxydisulfate, in an acidic solution such as 1 M HCl (Scheme 1).[9] This produces the acid doped, conductive emeraldine salt form that can then be dedoped by a base to yield the insulating emeraldine base form. The conductivity change between doped

---

Department of Chemistry and Biochemistry and California NanoSystems Institute, University of California, Los Angeles, Los Angeles, California, 90095-1569, USA. E-mail: kaner@chem.ucla.edu; Fax: (+1) 310 206 4038; Tel: (+1) 310 825 5346
† Current address: Department of Chemistry and Miller Institute for Basic Research in Science, University of California, Berkeley, California, 94720, USA.


Jiaxing Huang

Jiaxing Huang received his BS in chemistry from the University of Science and Technology of China (USTC) in 2000. He then joined University of California, Los Angeles (UCLA) as a graduate student, working with Professor Richard Kaner on conducting polymers and receiving his PhD in Inorganic Chemistry in 2004. He earned the 2005 International Union of Pure and Applied Chemistry (IUPAC) Young Chemist's Prize for "the best thesis in the chemical sciences", which includes the research described in this article. Currently he is a Miller Postdoctoral Fellow at UC Berkeley, where he is working with Professor Peidong Yang on patterning nanoparticles via controlled dewetting processes.

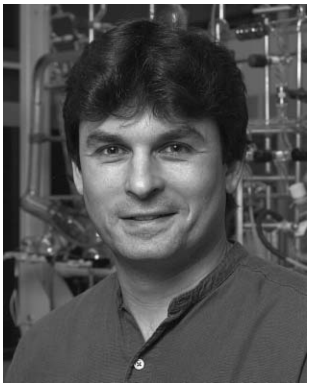
Richard B. Kaner

Richard B. Kaner is Professor of Chemistry and Professor of Materials Science and Engineering at UCLA. He received a PhD in inorganic chemistry from the University of Pennsylvania in 1984, followed by two and a half years of postdoctoral research at UC Berkeley. He joined UCLA in 1987 as an Assistant Professor, earned tenure in 1991 and became a full Professor in 1993. He has received awards from the Dreyfus, Fulbright, Guggenheim, Packard and Sloan Foundations for his work on new routes to refractory materials, including high temperature ceramics, intercalation compounds, fulleride superconductors, superhard materials and conducting polymers.

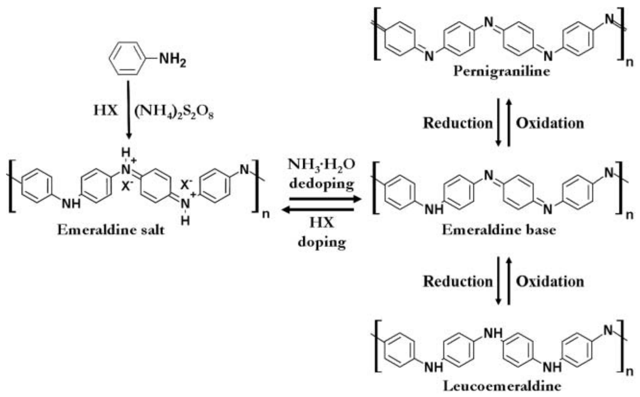

Scheme 1 The reversible acid/base doping/dedoping and redox chemistry of polyaniline. Chemical oxidative polymerization produces polyaniline in its emeraldine oxidation state. Dedoping with base creates the emeraldine base form. Reduction leads to leucoemeraldine while oxidation creates pernigraniline.

($\sigma \geqslant 1\ \mathrm{S\ cm^{-1}}$) and dedoped ($\sigma \leqslant 10^{-10}\ \mathrm{S\ cm^{-1}}$) states can be greater than ten orders of magnitude. Polyaniline possesses several intrinsic oxidation states:[12] the emeraldine base form is an intermediate oxidation state between pernigraniline, which is fully oxidized, and leucoemeraldine, which is fully reduced. Chemical or electrochemical means can be used to reversibly change the oxidation state. Electrochemical synthesis of polyaniline is also well known.[9] Since polyaniline is one of the most studied conducting polymers, there has been a great deal of interest in the past decade in making polyaniline nanostructures, especially as the field of nanoscience has taken-off.

Polyaniline nanostructures

Many methods have been described in the literature trying to shape polyaniline into nanostructures. At the individual nanostructural level, there are several methods for making polyaniline nanofibers, including templated polymerization in lithographically-defined nanochannels[13,14] or on single strands of DNA,[15,33] mechanical stretching,[16] and dip-pen writing[17] or drawing.[18] The capability of making polyaniline nanofibers individually at desired positions is needed to fabricate single nanofiber-based functional devices. At a slightly larger ''single substrate'' scale, polyaniline nanostructures can be made by confined polymerization within the voids in nanoporous membranes[4] or channels in zeolites[19] (Fig. 1a), by controlled electrochemical polymerization[20–22] or by electrospinning (Fig. 1c)[1,23–26] on conductive substrates. From a materials point of view, a bulk synthesis of nanostructured polyaniline may be more useful, since most current applications of polyaniline go far beyond individual nanostructures.

The most straightforward approach to making bulk quantities of nanostructured polyaniline is to introduce ''nanostructural directing agents'' during the chemical polymerization of aniline. These agents include surfactants,[27–30] liquid crystals,[31] polyelectrolytes,[32] nanowire seeds,[34] aniline oligomers[35] and complex, bulky dopants.[36–41] It has been suggested that these functional molecules can either directly act as templates (*e.g.* polyelectrolytes) or promote the self-assembly of ordered ''soft templates'' (*e.g.* micelles, emulsions) that guide the formation of polyaniline nanostructures (Fig. 1b). This Feature Article highlights a conceptually-new methodology that we have developed over the past three years that readily produces high quality, small diameter polyaniline nanofibers in large quantities.[42–44] In contrast to previous work, in which great effort was made to ''shape'' the polymer into nanostructures, our current work takes advantage of the nanofibrillar morphological unit that appears to be intrinsic to polyaniline[43] and focuses on modifying the reaction conditions so that nanofiber formation is favored, while overgrowth, that would otherwise lead to irregularly-shaped agglomerates, is suppressed. The availability of bulk polyaniline nanofibers has led to many exciting discoveries, including an unusual photothermal effect called ''flash welding'',[45] self-stabilizing aqueous colloidal suspensions that can be used to make ultra-thin films,[46] metal nanoparticle-decorated nanofibers for use in non-volatile flash memory devices,[47] as well as to improvements in conventional applications, such as in making highly responsive chemical vapor sensors.[42,48,49]

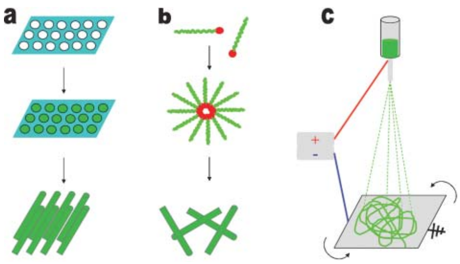

Fig. 1 Schematic illustration of different routes to conducting polymer nanostructures: (a) templated synthesis, (b) self-assembly using functional molecules and (c) electrospinning.

Intrinsic nanofibrillar morphology

Unlike inorganic materials, many polymeric materials are known to have well defined basic morphological units at the nanometer scale. For example, under proper synthetic conditions, fibers of 5 to 50 nm in diameter can be found in as-made polyacetylene films, the abundance of which are determined by the polymerization conditions.[50] It is known from the early years of conducting polymer research that polyaniline fibrils of $\sim$100 nm diameter can form ''naturally'' during electrochemical polymerization on the surface of the electrodes with a compact microspheroidal underlayer.[9] More recent work indicates that pure polyaniline nanofibers can be obtained without the need for any template, simply by controlling the electrochemical polymerization kinetics.[20–22] Since, in these reports, polyaniline nanofibers form without any structural directing agents, this suggests that the fibers of 10–100 nm diameter may be an intrinsic morphology that polyaniline possesses.

Chemical oxidative polymerization of aniline is the traditional method for preparing polyaniline in bulk. Green-colored polyaniline can be readily obtained after mixing aniline with an oxidant/initiator (typically ammonium peroxydisulfate) in an acidic solution. Because the oxidation of

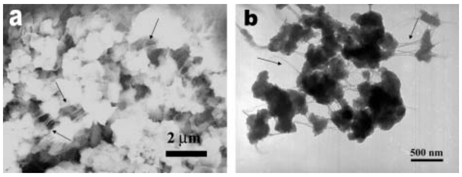

Fig. 2 Polyaniline powders made by traditional chemical polymerization reveal a small portion of nanofibers (arrows) in the sample *via* (a) SEM and (b) TEM images. [Reproduced with permission from *J. Am. Chem. Soc.*, 2004, **126**, 851–855. Copyright 2004 American Chemical Society]

aniline is exothermic, the oxidizing agent is often added slowly in a titration-type fashion in order to avoid increasing the temperature of the reaction mixture. Polyaniline prepared in this way is highly aggregated and rapid sedimentation from solution is generally observed. Examination using scanning (SEM) and transmission (TEM) electron microscopy shows that the as-synthesized polyaniline powders are mostly irregularly-shaped particles. However, careful examination reveals that a small quantity of nanofibers also appear in the product (Fig. 2). This has been confirmed recently in a SEM study on the morphology of high molecular weight polyaniline.[51] Apparently these nanofibers formed without any extra structural directing agents, again suggesting that nanofibers may be a natural morphology of polyaniline.

To investigate why the polymerization method affects the morphology of polyaniline, we revisited the conventional synthetic process for polyaniline.[9,43] This process has been employed for over 20 years, with little attention paid to the morphological evolution of polyaniline during chemical oxidative polymerization. A typical experiment is schematically illustrated in Fig. 3. The initiator solution is fed into the aniline solution using a syringe pump to gain better control over the reaction rate. The polyaniline product is then sampled periodically with a pipette from the reaction bath for examination under an electron microscope. Such aqueous extracts from the reaction are likely to contain polyaniline, and small molecules such as aniline oligomers, unreacted aniline and oxidant. In an electron microscopy study, these by-products, if present, would interfere strongly with the morphological observations. Additionally, the polymerization needs to be quenched as soon as possible to avoid the formation of new *ex situ* polyaniline. Therefore, special care has to be taken during sample preparation. These problems are solved by quickly diluting the reaction extract to the optimal concentration for TEM experiments and depositing it immediately onto sample grids placed on a piece of filter paper (Fig. 3, top right). In this way, the dilute extract is "filtered" through the microscopy grid and drained completely away by the underlying filter paper. The polyaniline product is trapped on the grid, and most of the water soluble reactants and by-products are absorbed by the filter paper.

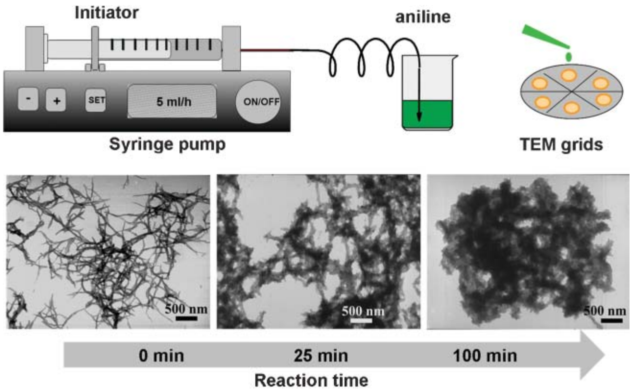

Fig. 3 Top: Schematic illustration of the experimental setup used to explore the morphological change of polyaniline during chemical polymerization. Bottom: TEM images showing the morphological evolution of polyaniline from nanofibers to agglomerates as the reaction proceeds. Time zero is defined as the moment that the green color of polyaniline becomes visible during the synthesis.

The TEM images of the product at different stages of the reaction are shown in Fig. 3, bottom. At a very early stage of the polymerization process, clean nanofibers with average diameters of 30–50 nm are obtained. As more ammonium peroxydisulfate solution is added into the aniline solution, the nanofibers become thicker and coarser, and the final reaction product contains mostly irregularly-shaped agglomerates (Fig. 3, bottom). These results indicate that the initial nanofibers formed may act as scaffolds for the overgrowth of irregularly-shaped polyaniline. Therefore, if the overgrowth of polyaniline can be suppressed after the initial nanofibrillar formation step, it should be possible to obtain a product of pure polyaniline nanofibers. This methodology is conceptually different from previous efforts that focused on shaping polyaniline into nanostructures. As described in the following sections, we have successfully developed two general approaches for synthesizing pure polyaniline nanofibers without the need for any extra structural directing agents—(1) interfacial polymerization and (2) rapidly-mixed reactions.

Interfacial polymerization

Polymer forming reactions that occur at the phase boundary of an immiscible aqueous/organic biphasic system are usually referred to as interfacial polymerizations.[52] Probably the most famous example is in the synthesis of Nylon.[53] When an aqueous solution of a diamine (*e.g.* hexamethylenediamine) and an organic solution of a diacid chloride (*e.g.* sebacyl chloride in chloroform) are brought together, they react to form a thin film of a polyamide, known as Nylon, at the interface between the aqueous and organic phases. Since Nylon is not soluble in either solvent, it blocks the mass transport across the interface and the polymerization stops. In a classroom demonstration, a stirring rod is typically used to pull a thick Nylon filament out from the interface thus creating fresh aqueous/organic interactions that lead to further polymerization. Hence a continuous Nylon fiber can be drawn until all the reactants are consumed (Fig. 4a). Now, contrast this with a typical interfacial polymerization reaction using the monomer aniline dissolved in an organic solvent and the oxidant ammonium peroxydisulfate dissolved in an aqueous acidic solution. Polyaniline forms at the interface, but unlike with Nylon, it diffuses into the water layer, leaving the interface available for further reaction (Fig. 4b).[42,44,48] This is

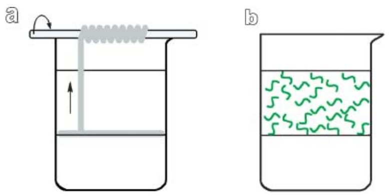

Fig. 4 Schematic illustrations of interfacial polymerization for (a) Nylon fibers and (b) polyaniline nanofibers. Both Nylon and polyaniline form at the interface, where all the reactants are available for polymerization. Since Nylon is insoluble in both solvents, it needs to be drawn out from the interface to allow further polymerization. Drawing or winding the Nylon produces a macrofilament. In contrast, polyaniline is produced in its doped hydrophilic form, which readily diffuses into the water layer, creating a fresh interface that allows the polymerization reaction to continue.

most likely due to the hydrophilic nature of the as-produced polyaniline, which forms in its doped, emeraldine salt state. Fig. 5 shows snapshots of a typical reaction. After a short induction period, ranging from seconds to several minutes, depending on the concentration of aniline and oxidants, green polyaniline appears at the interface (Fig. 5b). The polyaniline generated in this biphasic system migrates into the water phase and within minutes fills the entire water layer (Fig. 5c–f). As the reaction proceeds, the color of the organic phase becomes darker (Fig. 5f) and finally stops changing, indicating reaction completion. Note that the interfacially-polymerized polyaniline tends to disperse into the body of the aqueous solution after the reaction, while the polyaniline prepared by traditional polymerization usually precipitates out rapidly. The yield of polyaniline from interfacial polymerization is comparable to that by conventional synthesis with the same monomer-to-oxidant molar ratio. TEM analysis shows that the interfacial polymerization produces pure polyaniline nanofibers, typically with average diameters between 30–50 nm, as shown in Fig. 6a.

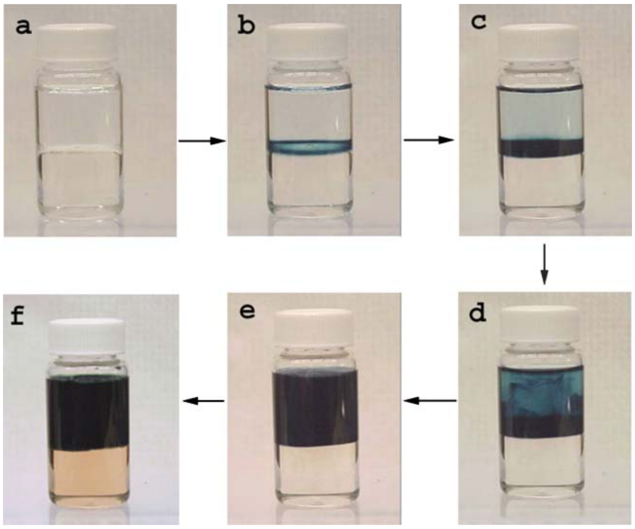

Fig. 5 Snapshots showing the interfacial polymerization of aniline. The reaction times are (a) 0 sec, (b) 60 sec, (c) 90 sec, (d) 120 sec, (e) 180 sec and (f) 2 h. The top layer is an aqueous solution of acid and oxidant; the bottom layer contains aniline dissolved in an organic solvent.

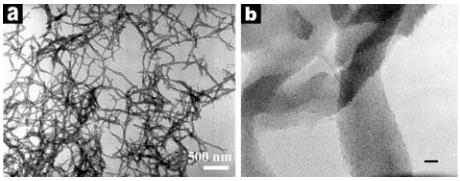

Fig. 6 (a) A typical TEM image showing polyaniline nanofibers obtained by interfacial polymerization. (b) A high resolution TEM image of polyaniline nanofibers. (Scale bar = 20 nm)

Ordering within individual nanofibers is not observed in high resolution TEM images (Fig. 6b), indicating that each nanofiber is composed of randomly packed polymer chains. Dedoping these nanofibers with a base does not appear to affect their morphology.

Interfacial polymerization represents an effective method of suppressing the overgrowth of polyaniline. Since the monomer aniline and the initiator ammonium peroxydisulfate are initially separated by the boundary between the aqueous and organic phases, polymerization occurs primarily at this interface—where all the components needed for polymerization come together (Fig. 5a,b). Based on the morphological evolution study, we now believe that when polyaniline first forms at the interface, it is in the form of pure nanofibers. In a conventional synthesis, these nanofibers are exposed immediately to unreacted monomer and initiator. In contrast, in an interfacial polymerization, these nanofibers rapidly move away from the interface and diffuse into the water layer, as shown in Fig. 5c–f. In this way, the nanofibers pull themselves away from the reaction front, thus avoiding overgrowth and allowing new nanofibers to grow at this interface. This also helps explain why nanofiber formation appears to be independent of the organic solvent used.

Rapidly-mixed reactions

Studying the morphological evolution during chemical oxidative polymerization indicates that the interface between the immiscible aqueous and organic layers does not contribute directly to nanofiber formation; it simply separates nanofiber formation from secondary overgrowth. Since polyaniline nanofibers are also observed in conventionally-synthesized products, there should be some conditions under which these nanofibers can avoid overgrowth. We have discovered a way to minimize the polyaniline overgrowth on these nanofibers by undertaking so-called ‘‘rapidly-mixed reactions’’. These can be achieved simply by pouring the initiator solution (*e.g.* ammonium peroxydisulfate) into the aniline solution all at once and rapidly mixing them (Fig. 7).[43] As the polymerization begins, the initiator molecules induce the formation of nanofibers by rapidly polymerizing aniline monomers in their vicinity. If the initiator molecules are evenly distributed, then they should be consumed during the formation of nanofibers. Therefore, secondary growth of polyaniline will be very limited due to a lack of available reactants. The effect of feeding rate on the polyaniline morphology is evident from Fig. 8. The product created in a rapidly-mixed reaction is pure nanofibers with a relatively uniform size distribution, comparable to that

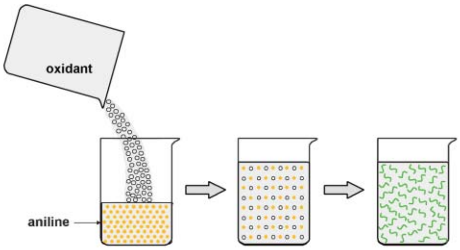

Fig. 7 A schematic illustration of polyaniline nanofiber synthesis in a rapidly-mixed reaction. (a) The oxidant (open circles) dopant solution is quickly added to the aniline (orange circles) dopant solution and mixed. (b) A homogenous solution is obtained where the aniline and oxidant molecules are evenly distributed, leading to rapid polymerization throughout the entire solution. (c) Since all the reactants are consumed in the formation of the nanofibers, secondary growth is suppressed.

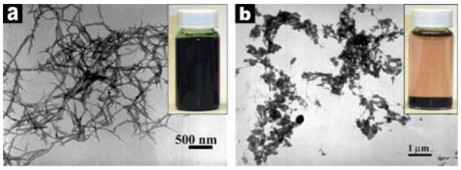

Fig. 8 TEM images showing the morphology of polyaniline synthesized by (a) a rapidly-mixed reaction and (b) a slowly-mixed reaction. High quality nanofibers are obtained in the rapidly-mixed reaction, while irregular agglomerates form in the slowly-mixed reaction. The insets show the as-prepared products in their reaction vials.

obtained by interfacial polymerization. On the other hand, the products from a slowly titrated reaction are irregularly-shaped agglomerates with very small quantities of nanofibers. The formation of nanofibers does not depend on the acid used in the synthesis, consistent with results from interfacial polymerization. Again it is worth noting that the as-synthesized nanofibers tend to disperse into the aqueous solution, while the product from a conventional slow mixing synthesis precipitates out after the stirring is stopped (Fig. 8 insets).

As mentioned earlier, the polymerization reaction of aniline is exothermic. Rapidly-mixed reactions are generally found to be warmer than slowly-mixed ones, most likely due to much faster reaction rates. Although heat is usually not a problem due to the large heat capacity of water, the reaction can start to get hot when the concentration of the initiator solution is increased to $\geqslant$1.0 M. To address the question of whether polyaniline nanofibers can still be obtained in hot reactions, a rapidly-mixed reaction was carried out in boiling water as shown in Fig. 9 (left). In this reaction, 1.0 M sulfuric acid was chosen as the doping acid due to its thermal stability. The monomer solution was first heated to boiling ($\sim$100 °C) and then the initiator solution was injected into the flask using a syringe. The reaction started upon injection and was allowed to boil at $\sim$100 °C for over 30 min. The observed product was also uniform nanofibers, suggesting that the heat generated from reactions should not be a problem to nanofiber formation.

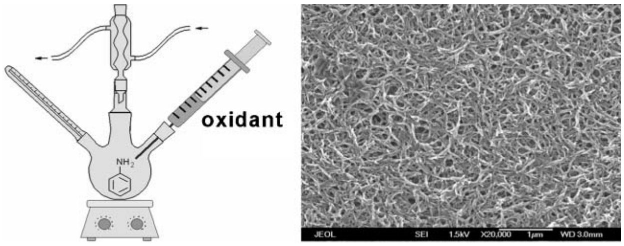

Fig. 9 Left: A schematic illustration showing an aniline polymerization reaction at 100 °C. Right: A SEM image of the morphology of the nanofiber product.

We have systematically adjusted the polymerization conditions to investigate what could affect the basic nanofibrillar morphology of polyaniline. It turns out that both interfacial polymerization and rapidly-mixed reactions are very robust syntheses that can be performed under a wide range of conditions, such as different reactant concentrations, temperatures and doping acids. Most of the experiments were carried out using ammonium peroxydisulfate ($(NH_4)_2S_2O_8$) as the oxidant. Other oxidants have also been tested; for example, iron trichloride ($FeCl_3$) also produces nanofibers of similar size and shape. However, when chloroauric acid ($HAuCl_4$) was used in rapidly-mixed reactions, thicker nanofibers with rougher surfaces were produced, with randomly distributed gold nanoparticles as a by-product of the polymerization reaction (Fig. 10). These results support the previous observation that a nanofibrillar morphology appears to be intrinsic to chemically-synthesized polyaniline, which can be made without any extra structural directing agents by interfacial polymerization or by rapidly-mixed reactions. In fact, both of these methods have now been confirmed by other groups as producing pure polyaniline nanofibers.[55–61]

Effects of dopants

In the aniline polymerization reaction, an acidic solution is needed to enhance the head-to-tail coupling between aniline monomers. Typically a strong mineral acid such as

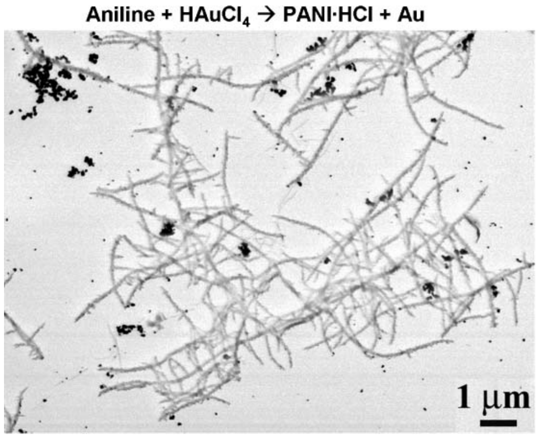

Fig. 10 TEM image showing the product from a rapidly-mixed reaction between aniline and $HAuCl_4$. Polyaniline nanofibers (light wires) and gold nanoparticles (dark spots) are obtained.

hydrochloric, sulfuric, nitric, perchloric or phosphoric is used at a high concentration ($\geqslant$1.0 M).[9] In both interfacial and rapidly-mixed reactions, pure polyaniline nanofibers are obtained with a wide range of acids (concentration = 1.0 M), including common mineral acids and organic acids such as formic, acetic, camphorsulfonic, methylsulfonic, 4-toluenesulfonic, ethylsulfonic or tartaric acid. For the mineral acids, if their concentration is reduced to below 0.001 M, sub-micron-sized particulates start to dominate the product morphology. When an amphiphilic organic acid such as camphorsulfonic is used at a low concentration, tube-like nanostructures with diameters of several hundred nanometers begin to appear in the product. This is consistent with previous reports on "dopant induced self-assembly", in which functional organic dopants are used, usually at concentrations orders of magnitude lower than 1.0 M, that are believed to self-assemble into micellular structures, guiding the formation of polyaniline nanotubes.[37,41,62,63]

The diameter of the nanofibers is strongly affected by the acid used in the polymerization.[44] For example, the average diameter of nanofibers produced with HCl is about 30 nm, while those made in camphorsulfonic acid approach 50 nm and those synthesized in perchloric acid are centered around 120 nm (Fig. 11). Other acids, including sulfuric, nitric and 4-toluenesulfonic, yield average diameters between 30 and 50 nm. When two dopant acids are used together in the synthesis, a mixture of two kinds of nanofibers are obtained rather than one. For example, mixing hydrochloric and camphorsulfonic acids produces nanofibers with average diameters around 30 and 50 nm, respectively, consistent with individual acid experiments.

The surface areas of the nanofibers are found to be diameter-dependant. Table 1 lists the surface areas of the nanofibers, measured with nitrogen adsorption–desorption isotherms using the Brunauer–Emmett–Teller (BET) method. For comparison, surface areas estimated using a nanocylindrical model are presented. As the nanofibers' diameters increase, their surface areas decrease, consistent with the estimated values. The measured values are higher than the estimated ones since the surfaces of the nanofibers are not as smooth as the surface of a perfect cylinder. Dedoping the nanofibers increases their surface area, most likely because of the increased free volume of the nanofibers, consistent with previous work on conventional polyaniline films.[64] The relatively high surface areas of the nanofibers may prove to be interesting for investigations of their gas absorption properties.

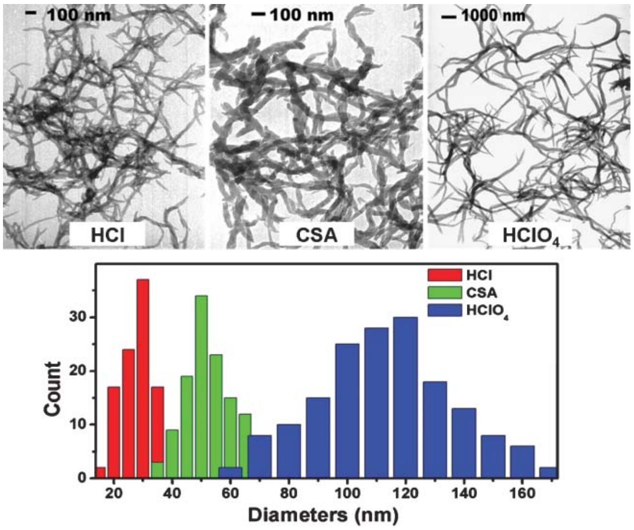

Fig. 11 TEM images (top) and diameter distributions (bottom) of the nanofibers made by interfacial polymerization using HCl (left), camphorsulfonic acid (CSA, middle) and $HClO_4$ (right), respectively. [Adapted with permission from *J. Am. Chem. Soc.*, 2004, **126**, 851–855. Copyright 2004 American Chemical Society]

Table 1 Experimental and calculated BET surface areas (S_A) of polyaniline nanofibers. The samples were de-gassed at 100 °C before measurement

Dopant:		HCl	CSA	$HClO_4$
Diameter/nm		30	50	120
Estimation/m^2 g^{-1}		51.3	30.8	12.8
BET S_A/m^2 g^{-1}	Doped	n/m[a]	41.2	34.2
	Dedoped	54.7	49.3	37.2

[a] n/m = Not measured. The HCl-doped nanofibers were not measured since residual HCl vapor released during de-gassing could have harmed the instrument.

Effects of solvents

The success of the above mentioned syntheses are based on the experimental observation that polyaniline nanofibers form at an early stage during polymerization. It is not completely clear why polyaniline forms such extended fibrillar structures. Note that the rapidly-mixed reactions can be carried out in solvents other than water. This makes it possible to investigate the impact of solvent on the basic polyaniline morphology. For example, rapidly-mixed reactions can be readily performed in alcohols such as methanol, ethanol and isopropanol since all the reactants: aniline, ammonium peroxydisulfate and hydrochloride acid are soluble in these short chain alcohols. It appears that the solvent's polarity strongly affects the product morphology. In water, pure nanofibers are obtained in a well-extended random network form (Fig. 8a). In methanol, thinner fibers (diameter < 30 nm) are obtained, but they are heavily entangled (Fig. 12a). In ethanol, the product is a mixture of

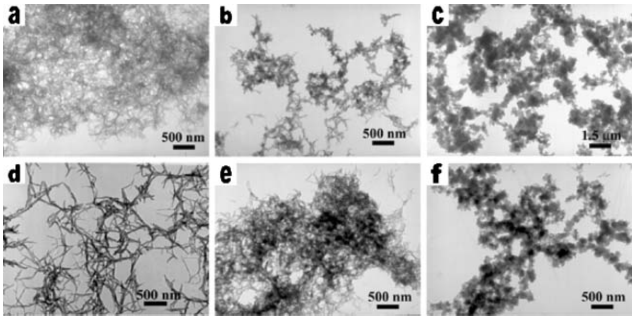

Fig. 12 TEM images showing the effects of different solvents on the basic morphology of polyaniline synthesized in (a) methanol, (b) ethanol, (c) isopropanol, (d) 9 : 1 water/isopropanol, (e) 5 : 5 water/isopropanol and (f) 1 : 9 water/isopropanol.

fibrillar structures and irregularly-shaped particles (Fig. 12b). In isopropanol, the morphology is dominated by irregular particles (Fig. 12c). This trend is confirmed by rapidly-mixed reactions in a solvent blend of water and isopropanol. In a 9 : 1 water/isopropanol mixture, the product resembles that obtained in pure water. However, as the fraction of isopropanol increases, the abundance of the nanofibers decreases significantly, and the nanofibers have essentially disappeared in a 1 : 9 water/isopropanol mixture. Water has so far proven to be the best solvent for making polyaniline nanofibers.

Although it is not clear yet how the solvent affects the organization of the polymer chains to produce different polymer morphologies, the current results are not surprising, based on polymer–solvent interactions. The as-synthesized polyaniline is in its hydrophilic, doped, emeraldine salt state. Therefore, well-extended nanofiber network structures are obtained in water, since they are provided with enhanced interactions with the aqueous environment. In a less polar solvent, such as isopropanol, the polymer may associate better with itself than with the solvent, and therefore form compact aggregates. In a polyaniline synthesis, each nanofiber consists of a collection of randomly-packed polyaniline chains that polymerized from monomers. There should be a transition from monomer, to polymer, to fiber during the reaction. This process may be difficult to probe directly during a polymerization reaction. However, some attempts have been made to probe the process indirectly. For example, when camphorsulfonic acid (CSA) doped polyaniline is blended in a host polymer such as poly(methyl methacrylate), the composite materials can be made electrically conductive, even when there is only 2 wt% of polyaniline. This low percolation threshold made sense after an interpenetrating network-like structure was revealed, composing of polyaniline nanofiber ''linkers'' with diameters of a few tens of nanometers.[65] When the polyaniline powders are dissolved in an organic solvent during the blending process, the polymer particles are disassembled to the level of individual polymer chains. Apparently, the final nanofiber linkers are formed through a ''re-assembly'' process, in which nanofiber formation is favored by the surrounding chemical environment. Inspired by this idea, we carried out the following experiment to mimic the re-assembly process in polyaniline composites. Firstly, a polyaniline solution was prepared by dissolving conventionally-synthesized polyaniline emeraldine base particles into *N*-methyl-2-pyrrolidone (NMP), which is a widely-used good solvent for polyaniline. This should disentangle the polymer chains and destroy any structure that the particles may have possessed. Then, a small amount of this solution (1 ml) was added into a 1 M CSA aqueous solution (20 ml) and polyaniline precipitated out from it. This re-assembly process indeed produced polyaniline networks with short nano linkers having diameters around 50 nm (Fig. 13). These nano linkers and the network were not perfect, but they strongly resembled the nanofibers obtained from a bottom-up synthesis in terms of their size and shape. This suggests the possibility of producing polyaniline nanostructures by simply using solvent exchange to find the optimal solvent–polymer interactions for nanofiber production. In fact, this re-assembly process has been demonstrated to create polyaniline nanofibers by wrapping polyaniline chains together with a natural polysaccharide, schizophyllan.[66] Many further successful examples can also be found with other conducting polymers, especially regioregular polythiophenes.[67]

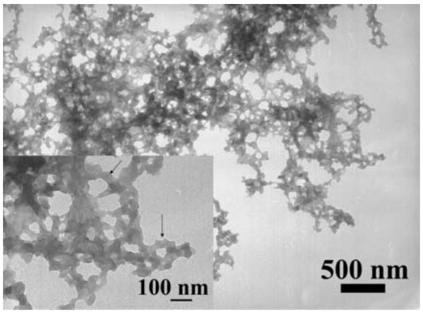

Fig. 13 A TEM image showing the morphology of polyaniline precipitates formed when 1 ml of a polyaniline/NMP solution was added to 20 ml of an aqueous solution of 1 M CSA. The inset shows a higher magnification image.

Purification and processibility

The as-prepared nanofibers can be purified by common solid–liquid separation techniques such as filtration, dialysis or centrifugation. As the first step in the processing history of the nanofibers, we have noticed that the purification method affects their further processibility in solvents and ultimately their device performance. Therefore, we believe it is necessary to discuss this seemingly trivial question, but one which becomes most important in practical applications. Note that when polyaniline nanofibers are processed in a solvent, there are two levels of processibility at different length scales. As with conventional polyaniline, polyaniline nanofibers can be ''dissolved'' in a good solvent (*e.g.* *N*-methyl-2-pyrrolidone or *meta*-cresol) to form a dispersion of individual polymer chains or agglomerates, in which their nanofibrillar morphology is lost. More importantly, colloidal dispersions of nanofibers in a non-solvent (*e.g.* water) can be made that retain the nanofibrillar morphology, thus enabling further processing. In applications that require thin films of nanofibers, the quality of the nanofibrillar films is dictated by the quality of the dispersions they are cast from.

Filtration seems to be the fastest way to purify polyaniline nanofibers. In gram scale syntheses, the product can be readily vacuum filtered using common cellulose filter papers with negligible loss. Polyaniline nanofibers are obtained in powder form after drying the filter cake. The dry powders of polyaniline can be redispersed in a solvent using mild sonication, and their dispersity is much improved compared to conventional polyaniline powders. However, most likely due to the pressure generated during the filtering process, the redispersed polyaniline particles are composed of heavily agglomerated nanofibers (Fig. 14).

Dialysis and centrifugation both yield well dispersed nanofibers, such as those shown in Fig. 5. Dispersions prepared in this fashion are stable from hours to days, depending the concentration of the nanofibers. Dialysis is

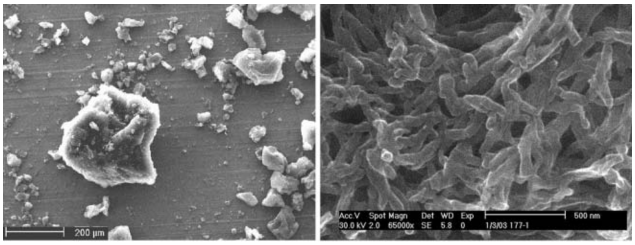

Fig. 14 Polyaniline powders obtained after filtration. SEM images show that the powders (left) are agglomerations of nanofibers (right). [Reproduced with permission from *J. Am. Chem. Soc.*, 2004, **126**, 851–855. Copyright 2004 American Chemical Society]

suitable for relatively small scale synthesis since there is essentially no product lost—the crude product is sealed in the dialysing tubing during dialysis. Centrifugation is more versatile for solvent exchange, however, it appears to cause the most product loss, as we noticed that the color of the supernatant became more intense after a couple of centrifugation cycles, indicating an increased concentration of nanofibers in the supernatant. The stability of the supernatant against centrifugation has led to the recent discovery that polyaniline nanofibers can form self-stabilizing colloids in water at a pH value around 2.6.[46] (Fig. 15). Such colloids are especially useful in preparing nanofiber monolayers (Fig. 16) on a charged substrate in a "layer-by-layer" fashion,[68] since each doped polyaniline nanofiber can be viewed as a positively-charged polyelectrolyte with counterions around its backbone.

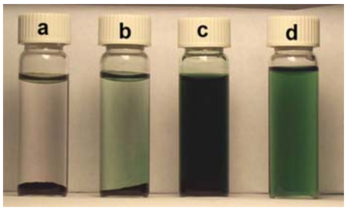

Fig. 15 (a) As-polymerized polyaniline nanofibers after washing with water and centrifugation at 3 000 rpm for 0.5 h, flocculated out of water. (b) After washing/centrifuging a second time, the green color of the emeraldine salt becomes visible. (c) After washing/centrifuging a third time, a thick dispersion is obtained. The green color of the dispersed emeraldine salt form of polyaniline becomes visible after diluting 1 ml of the supernatant from (c) with 4 ml of 0.005 M HCl to form (d). [Reproduced with permission from *Chem. Commun.*, 2005, 3286. Copyright 2005 Royal Society Chemistry]

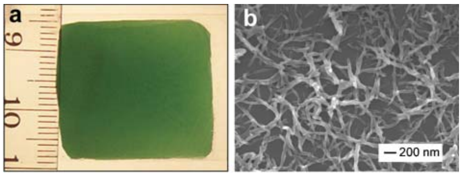

Fig. 16 (a) A high quality polyaniline nanofiber thin film is cast on a glass slide from a HCl-doped nanofiber colloidal solution. (b) A SEM image of a nanofiber monolayer adsorbed on a silicon wafer after immersing the wafer into the colloidal solution. [Reproduced with permission from *Chem. Commun.*, 2005, 3286. Copyright 2005 Royal Society Chemistry]

Preliminary experiments indicate that it is also possible to make stable nanofiber colloidal suspensions in organic solvents stabilized by organic dopants such as camphorsulfonic acid or 4-toluenesulfonic acid.

Polyaniline derivatives

Substituted polyanilines continue to be of great interest since they can improve upon some of the properties of polyaniline.[7] For example, compared with conventional polyaniline, improved processibility has been demonstrated with alkyl-substituted polyanilines.[69,70] Additionally, fluoro-substituted polyanilines have been reported as more stable against microbial and chemical degradation,[71–75] and are therefore being examined for several bio-related applications, such as bacterial based fuel cells. Many of these aniline derivatives, such as toluidine, anisidine, ethylaniline and fluoroaniline, can be polymerized using oxidative polymerization reactions under conditions very similar to aniline polymerization.[7,70,73–78] Therefore, the synthetic methods we have developed for making polyaniline nanofibers should also be very useful for studying the basic morphology of these polyaniline derivatives.

We have investigated the effects of substituent groups on the basic morphology of polyaniline derivatives prepared using both interfacial polymerization and rapidly-mixed reactions. It was found that both the substituent groups and their positions

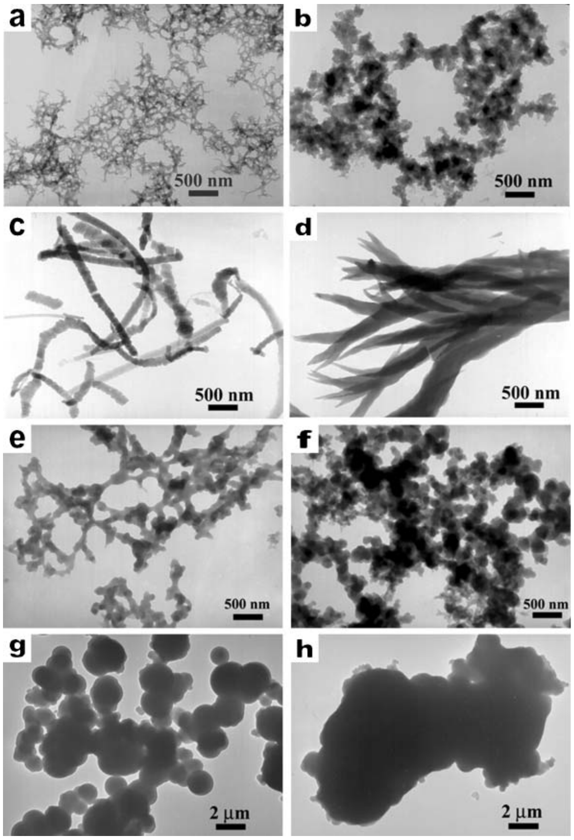

Fig. 17 TEM images show distinct morphological differences between *meta*- (left column) and *ortho*- (right column) substituted (a,b) polytoluidines, (c,d) polyfluoroanilines, (e,f) polyethylanilines and (g,h) polyanisidines.

on the monomer strongly affect the morphology. The TEM images in Fig. 17 show the typical morphology of *ortho*- and *meta*-substituted polyaniline derivatives synthesized by rapidly-mixed reactions. Note that while the polymers from *ortho*- and *meta*-substituted aniline monomers are essentially identical in chemical structure,[75] their morphologies are drastically different. The *ortho*-substituted derivatives tend to form larger and less well-ordered structures than their *meta*-substituted counterparts. Fibrillar structures are observed in *meta*-substituted polytoluidine, polyfluoroaniline and polyethylaniline.

Conclusions and outlook

We have discovered that the spontaneous formation of polyaniline nanofibers occurs during the early stages of chemical oxidative polymerization of aniline in water. A nanofibrillar morphology appears to be intrinsic to polyaniline synthesized in water. Two approaches—interfacial polymerization and rapidly-mixed reactions—have been invented to make pure nanofibers by suppressing the secondary growth of polyaniline, which would otherwise produce irregularly-shaped particles, as observed in conventional synthesis. The change in morphology significantly improves the solvent processibility of polyaniline.

The chemical and physical properties of the nanofibers, *i.e.* crystallinity, electrical conductivity and molecular weight distribution, are comparable to conventional particulate polyaniline.[44] However, the uniform, small size and high surface area of the nanofibers *vis-à-vis* conventional polyaniline, predict that they should have improved performance in devices, especially where a high interface area between polyaniline and its environment is useful; for example, when polyaniline is used as the selective layer in chemical vapor sensors, the vapor–polymer interaction is facilitated by its nanofiber structure. Polyaniline nanofiber thin films are found to outperform conventional polyaniline thin films with higher sensitivities and faster response times.[18,42,48,49,79,80] The porous open structure of polyaniline thin films also dramatically reduces the effect of film thickness on their performance, since their surface area is determined by the diameter of the nanofibers rather the thickness of the films.[42,48] On the other hand, the excellent water dispersity of the nanofibers renders improved interactions with ions in solution. This enables polyaniline nanofibers to be uniformly modified to render improved, and even new, functionalities that conventional polyaniline does not possess. One example is a new mechanism for detecting hydrogen sulfide gas using metal salt-modified polyaniline nanofibers.[79] Another example is the creation of uniform metal nanoparticle–polyaniline nanofiber composites for applications in non-volatile, electrically-bistable, memory devices.[47] The polymeric nature of these nanofibers also generate some interesting properties that may not be available to inorganic nanowires. For example, we have also observed an enhanced photothermal effect with these polyaniline nanofibers, and have developed a flash welding technique to join them together using a camera flash.[45]

The polyaniline nanofiber syntheses described here are very facile and robust. They do not require any extra structural directing agents or template removing steps. Together with the exciting properties and applications of polyaniline, we hope that this article will encourage the exploration of polyaniline nanofibers for many other applications, since essentially anyone who knows how to make polyaniline will now know how to make high quality polyaniline nanofibers.[54]

Acknowledgements

We thank J. R. Moore, K. N. Tun and G. J. Tong for technical assistance, and Dr. D. Li for helpful discussions. This work has been generously supported by the Microelectronics Advanced Research Corporation (MARCO) and its focus center on Functional Engineered NanoArchitectonics (FENA), and the National Science Foundation Nanoscale Integrated Research Team award DMR-0507294.

References

1 D. H. Reneker and I. Chun, *Nanotechnology*, 1996, **7**, 216–223.
2 R. Dersch, M. Steinhart, U. Boudriot, A. Greiner and J. H. Wendorff, *Polym. Adv. Technol.*, 2005, **16**, 276–282.
3 T. Ochi, *Cellul. Commun.*, 2004, **11**, 67–70.
4 C. R. Martin, *Acc. Chem. Res.*, 1995, **28**, 61–68.
5 M. J. Sailor and C. L. Curtis, *Adv. Mater.*, 1994, **6**, 688–692.
6 G. G. Wallace and P. C. Innis, *J. Nanosci. Nanotechnol.*, 2002, **2**, 441–451.
7 P. Chandrasekhar, *Conducting Polymers, Fundamentals and Applications: A Practical Approach*, Kluwer Academic Publishers, Boston, 1999.
8 T. J. Skotheim, R. L. Elsenbaumer and J. R. Reynolds, *Handbook of Conducting Polymers*, Marcel Dekker, New York, 1998.
9 W. S. Huang, B. D. Humphrey and A. G. MacDiarmid, *J. Chem. Soc., Faraday Trans. 1*, 1986, **82**, 2385–2400.
10 A. G. MacDiarmid, J. C. Chiang, M. Halpern, W. S. Huang, S. L. Mu, N. L. D. Somasiri, W. Q. Wu and S. I. Yaniger, *Mol. Cryst. Liq. Cryst.*, 1985, **121**, 173–180.
11 A. G. MacDiarmid, *Synth. Met.*, 1997, **84**, 27–34.
12 E. T. Kang, K. G. Neoh and K. L. Tan, *Prog. Polym. Sci.*, 1998, **23**, 277–324.
13 K. Ramanathan, M. A. Bangar, M. Yun, W. Chen, A. Mulchandani and N. V. Myung, *Nano Lett.*, 2004, **4**, 1237–1239.
14 M. Yun, N. V. Myung, R. P. Vasquez, J. Wang and H. Monbouquette, *Proc. SPIE-Int. Soc. Opt. Eng.*, 2003, **5220**, 37–45.
15 Y. Ma, J. Zhang, G. Zhang and H. He, *J. Am. Chem. Soc.*, 2004, **126**, 7097–7101.
16 H. X. He, C. Z. Li and N. J. Tao, *Appl. Phys. Lett.*, 2001, **78**, 811–813.
17 P. Xu and D. L. Kaplan, *Adv. Mater.*, 2004, **16**, 628–633.
18 H. Liu, J. Kameoka, D. A. Czaplewski and H. G. Craighead, *Nano Lett.*, 2004, **4**, 671–675.
19 C. G. Wu and T. Bein, *Science*, 1994, **264**, 1757–1759.
20 S. J. Choi and S. M. Park, *J. Electrochem. Soc.*, 2002, **149**, E26–E34.
21 J. Liu, Y. H. Lin, L. Liang, J. A. Voigt, D. L. Huber, Z. R. Tian, E. Coker, B. Mckenzie and M. J. McDermott, *Chem.–Eur. J.*, 2003, **9**, 605–611.
22 L. Liang, J. Liu, C. F. Windisch, G. J. Exarhos and Y. H. Lin, *Angew. Chem., Int. Ed.*, 2002, **41**, 3665–3668.
23 A. G. MacDiarmid, W. E. Jones, I. D. Norris, J. Gao, A. T. Johnson, N. J. Pinto, J. Hone, B. Han, F. K. Ko, H. Okuzaki and M. Llaguno, *Synth. Met.*, 2001, **119**, 27–30.
24 K. Desai and C. Sung, *Mater. Res. Soc. Symp. Proc.*, 2002, **736**, 121–126.
25 K. Desai and C. Sung, *Mater. Res. Soc. Symp. Proc.*, 2003, **788**, 209–214.
26 N. J. Pinto, A. T. Johnson, Jr, A. G. MacDiarmid, C. H. Mueller, N. Theofylaktos, D. C. Robinson and F. A. Miranda, *Appl. Phys. Lett.*, 2003, **83**, 4244–4246.

27 J. C. Michaelson and A. J. McEvoy, *J. Chem. Soc., Chem. Commun.*, 1994, 79–80.

28 L. Yu, J. I. Lee, K. W. Shin, C. E. Park and R. Holze, *J. Appl. Polym. Sci.*, 2003, **88**, 1550–1555.

29 G. Li and Z. Zhang, *Macromolecules*, 2004, **37**, 2683–2685.

30 X. Zhang and S. K. Manohar, *Chem. Commun.*, 2004, **20**, 2360–2361.

31 L. M. Huang, Z. B. Wang, H. T. Wang, X. L. Cheng, A. Mitra and Y. X. Yan, *J. Mater. Chem.*, 2002, **12**, 388–391.

32 J. M. Liu and S. C. Yang, *J. Chem. Soc., Chem. Commun.*, 1991, 1529–1531.

33 Y. Shao, Y. Jin and S. Dong, *Electrochem. Commun.*, 2002, **4**, 773–779.

34 X. Zhang, W. J. Goux and S. K. Manohar, *J. Am. Chem. Soc.*, 2004, **126**, 4502–4503.

35 W. G. Li and H. L. Wang, *J. Am. Chem. Soc.*, 2004, **126**, 2278–2279.

36 M. X. Wan, in *Encyclopedia of Nanoscience and Nanotechnology*, ed. H. S. Nalwa, American Scientific Publishers, Los Angeles 2004, vol. 2, pp. 153–169.

37 Z. X. Wei, Z. M. Zhang and M. X. Wan, *Langmuir*, 2002, **18**, 917–921.

38 P. J. Kinlen, J. Liu, Y. Ding, C. R. Graham and E. E. Remsen, *Macromolecules*, 1998, **31**, 1735–1744.

39 Z. X. Wei and M. X. Wan, *J. Appl. Polym. Sci.*, 2003, **87**, 1297–1301.

40 J. J. Langer, G. Framski and R. Joachimiak, *Synth. Met.*, 2001, **121**, 1281–1282.

41 H. J. Qiu, M. X. Wan, B. Matthews and L. M. Dai, *Macromolecules*, 2001, **34**, 675–677.

42 J. X. Huang, S. Virji, B. H. Weiller and R. B. Kaner, *J. Am. Chem. Soc.*, 2003, **125**, 314–315.

43 J. X. Huang and R. B. Kaner, *Angew. Chem., Int. Ed.*, 2004, **43**, 5817–5821.

44 J. X. Huang and R. B. Kaner, *J. Am. Chem. Soc.*, 2004, **126**, 851–855.

45 J. X. Huang and R. B. Kaner, *Nat. Mater.*, 2004, **3**, 783–786.

46 D. Li and R. B. Kaner, *Chem. Commun.*, 2005, 3286–3288.

47 R. J. Tseng, J. X. Huang, J. Ouyang, R. B. Kaner and Y. Yang, *Nano Lett.*, 2005, **5**, 1077–1080.

48 J. X. Huang, S. Virji, B. H. Weiller and R. B. Kaner, *Chem.–Eur. J.*, 2004, **10**, 1314–1319.

49 S. Virji, J. X. Huang, R. B. Kaner and B. H. Weiller, *Nano Lett.*, 2004, **4**, 491–496.

50 J. C. W. Chien, Y. Yamashita, J. A. Hirsch, J. L. Fan, M. A. Schen and F. E. Karasz, *Nature*, 1982, **299**, 608–611.

51 D. Chao, J. Chen, X. Lu, L. Chen, W. Zhang and Y. Wei, *Synth. Met.*, 2005, **150**, 47–51.

52 E. L. Wittbecker and P. W. Morgan, *J. Polym. Sci., Part A: Polym. Chem.*, 1996, **34**, 521–529.

53 P. W. Morgan and S. L. Kwolek, *J. Chem. Educ.*, 1959, **36**, 182–184.

54 E. K. Wilson, *Chem. Eng. News*, 2005, **83**, 37.

55 P. L. B. Araujo, E. S. Araujo, R. F. S. Santos and A. P. L. Pacheco, *Microelectron. J.*, 2005, **36**, 1055–1057.

56 Y. He, *Mater. Sci. Eng., B*, 2005, **122**, 76–79.

57 A. R. Hopkins, D. D. Sawall, R. M. Villahermosa and R. A. Lipeles, *Thin Solid Films*, 2004, **469–470**, 304–308.

58 X. Zhang, R. Chan-Yu-King, A. Jose and S. K. Manohar, *Synth. Met.*, 2004, **145**, 23–29.

59 J. Jang, J. Bae and K. Lee, *Polymer*, 2005, **46**, 3677–3684.

60 N.-R. Chiou and A. J. Epstein, *Adv. Mater.*, 2005, **17**, 1679–1683.

61 R. C. Y. King and F. Roussel, *Synth. Met.*, 2005, **153**, 337–340.

62 Z. X. Wei and M. X. Wan, *Adv. Mater.*, 2002, **14**, 1314–1317.

63 H. J. Qiu and M. X. Wan, *J. Polym. Sci., Part A: Polym. Chem.*, 2001, **39**, 3485–3497.

64 M. R. Anderson, B. R. Mattes, H. Reiss and R. B. Kaner, *Science*, 1991, **252**, 1412–1415.

65 C. Y. Yang, Y. Cao, P. Smith and A. J. Heeger, *Synth. Met.*, 1993, **53**, 293–301.

66 M. Numata, T. Hasegawa, T. Fujisawa, K. Sakurai and S. Shinkai, *Org. Lett.*, 2004, **6**, 4447–4450.

67 J. A. Merlo and C. D. Frisbie, *J. Polym. Sci., Part B: Polym. Phys.*, 2003, **41**, 2674–2680.

68 G. Decher, *Science*, 1997, **277**, 1232–1237.

69 A. Gruger, A. Novak, A. Regis and P. Colomban, *J. Mol. Struct.*, 1994, **328**, 153–167.

70 S. M. Yang and J. H. Chiang, *Synth. Met.*, 1991, **41**, 761–764.

71 J. Niessen, U. Schroder, M. Rosenbaum and F. Scholz, *Electrochem. Commun.*, 2004, **6**, 571–575.

72 A. L. Sharma, S. Annapoorni and B. D. Malhotra, *Curr. Appl. Phys.*, 2003, **3**, 239–245.

73 A. L. Sharma, M. Gerard, R. Singhal, B. D. Malhotra and S. Annapoorni, *Appl. Biochem. Biotechnol.*, 2001, **96**, 155–165.

74 A. Cihaner and A. M. Onal, *Eur. Polym. J.*, 2001, **37**, 1767–1772.

75 A. H. Kwon, J. A. Conklin, M. Makhinson and R. B. Kaner, *Synth. Met.*, 1997, **84**, 95–96.

76 A. L. Sharma, V. Saxena, S. Annapoorni and B. D. Malhotra, *J. Appl. Polym. Sci.*, 2001, **81**, 1460–1466.

77 E. P. Koval'chuk, N. V. Stratan, O. V. Reshetnyak, J. Blazejowski and M. S. Whittingham, *Solid State Ionics*, 2001, **141**, 217–224.

78 L. X. Wang, X. B. Jing and F. S. Wang, *Synth. Met.*, 1991, **41**, 745–748.

79 S. Virji, J. D. Fowler, C. O. Baker, J. Huang, R. B. Kaner and B. H. Weiller, *Small*, 2005, **1**, 624–627.

80 B. Ding, J. Kima, Y. Miyazaki and S. Shiratori, *Sens. Actuators, B*, 2004, **101**, 373–380.